CONF-950472--8

UCRL-JC-120745
PREPRINT

A Lightweight High Performance Dual-Axis Gimbal for Space Applications

D. J. Pines
D. B. Hakala
R. Malueg

This paper was prepared for submittal to the
SPIE International Symposium of Aerospace/Defense
Sensing and Control and Dual-Use Phontonics
Orlando, FL
April 17-21, 1995

May 5, 1995

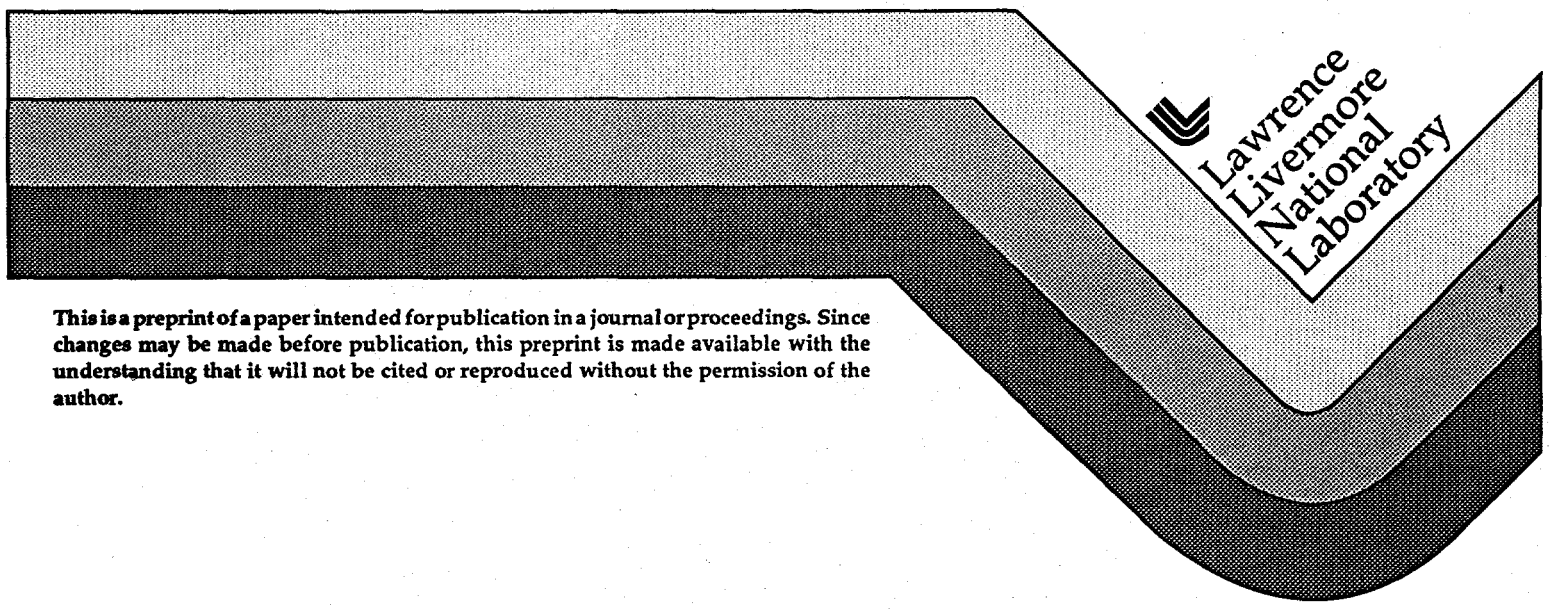

This is a preprint of a paper intended for publication in a journal or proceedings. Since changes may be made before publication, this preprint is made available with the understanding that it will not be cited or reproduced without the permission of the author.

DISCLAIMER

This document was prepared as an account of work sponsored by an agency of the United States Government. Neither the United States Government nor the University of California nor any of their employees, makes any warranty, express or implied, or assumes any legal liability or responsibility for the accuracy, completeness, or usefulness of any information, apparatus, product, or process disclosed, or represents that its use would not infringe privately owned rights. Reference herein to any specific commercial product, process, or service by trade name, trademark, manufacturer, or otherwise, does not necessarily constitute or imply its endorsement, recommendation, or favoring by the United States Government or the University of California. The views and opinions of authors expressed herein do not necessarily state or reflect those of the United States Government or the University of California, and shall not be used for advertising or product endorsement purposes.

DISCLAIMER

Portions of this document may be illegible in electronic image products. Images are produced from the best available original document.

A Lightweight High Performance Dual-Axis Gimbal for Space Applications

Darryll J. Pines
Department of Aerospace Engineering
University of Maryland
College Park, Maryland

Dennis B. Hakala
Electrical Engineering Department
Lawrence Livermore National Laboratory
Livermore, California

Richard Malueg
Richard Malueg, Inc.
Santa Ana, California

ABSTRACT

This paper describes the design, development and performance of a lightweight precision gimbal with dual-axis slew capability to be used in a closed-loop optical tracking system at Lawrence Livermore National Laboratory-LLNL. The motivation for the development of this gimbal originates from the need to acquire and accurately loacalize warm objects (T~500 K) in a cluttered background. The design of the gimbal is centered around meeting the following performance requirements:

Pointing Accuracy with control < 35 μrad-(1-σ)
Slew Capability > 0.2 rad/sec
Mechanical Weight < 5 kg

These performance requirements are derived by attempting to track a single target from multiple satellites in low Earth orbit using a mid-wave infrared camera. Key components in the gimbal hardware that are essential to meeting the performance objectives include a nickel plated beryllium mirro, an accurate lightweight capacitive pickoff device for angular measurement about the elevation axis, a 16-bit coarse/fine resolver for angular measurement about the azimuth axis, a toroidally wound motor with low hysteresis for providing torque about the azimuth axis, and the selection of beryllium parts to insure high stiffness to weight ratios and more efficient thermal conductivity. Each of these elements are discussed in detail to illustrate the design trades performed to meet the tracking and slewing requirements demanded. Preliminary experimental results are also given for various commanded tracking maneuvers.

1.0 INTRODUCTION

There are many terrestrial and non-terrestrial applications in which the ability to point camera assets on demand is required. Some of these terrestrial applications include tracking forest fires, monitoring pollution spills and tracking criminal activity. Aerial platforms which permit this monitoring include Unmanned[1] and Manned Aerial Vehicles-(UAVs, MAV). Non-terrestrial applications which require the ability to point on demand include satellite tracking for science and defense objectives.[2] The LLNL dual-axis gimbal discussed in this paper is intended to address these objectives. LLNL has leveraged

DISTRIBUTION OF THIS DOCUMENT IS UNLIMITED
MASTER

experience gained in developing space-qualified cameras for the Clementine Program to aid in the design of a space-qualified dual-axis gimbal which can point accurately and on demand. As in the case of the Clementine sensors, commercial-grade components were used to take advanteage of the latest technology and reduce costs but were screened to standards for space applications to ensure that they would operate successfully in a LEO environment.[3]

The environmental specifications used to provide guidance for designing the gimbal mechanical and electrical components are summarized below for temperature, radiation and quasi-static launch vehicle loads:

Temperature:

- gimbal mirror operating temperature-(-43 to 10 deg C ± 5 deg C)
- on-orbit operating temperature for electronics mounted on payload bench-(0 to 10 deg C)

Radiation:

- must tolerate 20 krads total dose consisting of trapped protons, trapped electrons, Cosmic rays, and solar protons (analysis parameters include: 60 mil Al; absorption in Si; 400 km altitude orbit at 45 degree inclination)

Quasi-Static Acceleration Requirement:

Test Type	Limit Load	Acceptance Load	Protoflight Load	Prototype Qual Load
Loading Direction				
Perpendicular to mounting surface (Z)	± 10.6 g's	± 10.6 g's	± 16 g's	± 16 g's
Parallel to mounting surface (X)	± 10.6 g's	± 10.6 g's	± 16 g's	± 16 g's
Parallel to mounting surface (Y)	± 10.6 g's	± 10.6 g's	± 16 g's	± 16 g's

In addition to these environmental performance specifications, the gimbal also had to meet specific pointing/slewing performance requirements for tracking warm objects against a cluttered background. These pointing requirements are discussed next in section 2.0. Section 3.0 discusses key aspects of the gimbal design that were essential for meeting the environmental specifications and performance requirements of section 1.0 and 2.0 respectively. Preliminary laboratory using the prototype gimbal results are discussed in section 4.0.

2.0 GIMBAL PERFORMANCE REQUIREMENTS

Pointing and slewing requirements are driven by several system-level factors which begin with the top level mission requirements. In this case, the objective was to acquire and localize warm objects as accurately as possible. System parameters which affect this requirement include the satellite orbit-(altitude, inclination, range to target), the tracking sensor's characteristics, the relative Line-of-Sight (LOS) knowledge, and the hand-off requirements for transferring the track data off to other assets. In general, requirements for tracking are that the satellite's sensor must have the target in its field-of-view (FOV) and the system software must be able to locate the target when it is in the sensor's FOV to some level of accuracy.

A generic set of 1-sigma mission requirements (see Fig. 1) were used to help fold down specific requirements for the lightweight gimbal design discussed in this paper. This set is based on several

proposed warm body tracking experiments and convergence of various Kalman filter designs on relative target position and velocity under mono and stereo satellite observation. The parameters used to help define these generic mission requirements are summarized below in Table 1:

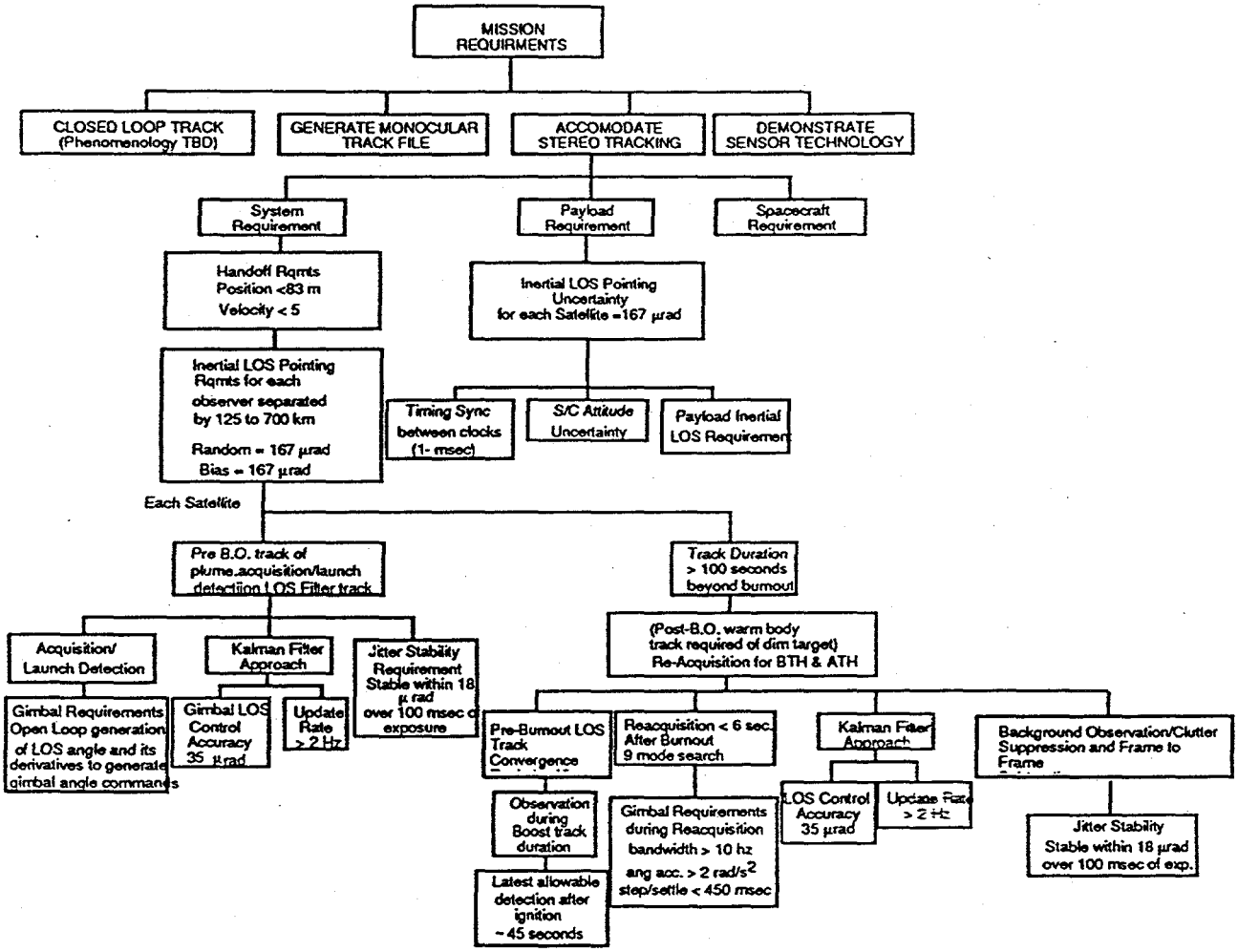

Figure 1: One-σ Mission Requirements for Tracking from a LEO Satellite

Table 1: Parameters used to define generic mission requirements for warm-body tracking.

Orbit: 400 km altitude, 45 degree inclination
Sensor: Sensitivity in the mid-wave infrared
pixel size: 50 to 80 µrad
array size: 256x256
FOV: 14 mrad to 20.5 mrad
minimum range to target: 400 km

The LOS pointing requirements follow from the general mission requirement to track warm bodies to some level of accuracy in position and velocity. Figure 2 summarizes how top level mission requirements flow down into requirements for the payload and finally the gimbal line-of-sight pointing accuracy. The two sets of angle numbers are estimates for random and bias angular errors. Slewing requirements follow from how fast the target is moving relative to the instrument performing the tracking function.

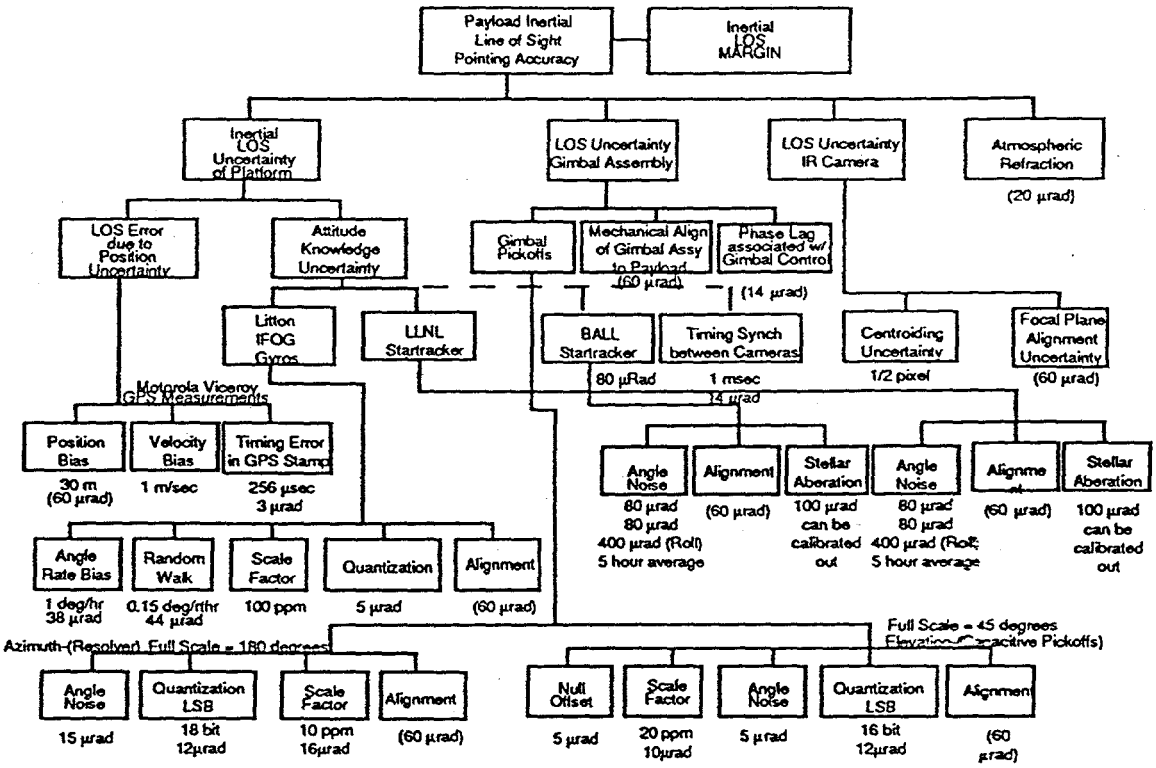

Figure 2: 1-σ Requirements Flowdown for one observer used in a Dual-Observer tracking mode

Table 2 summarizes the gimbal performance requirements for meeting typical mission objectives:

Table 2: Gimbal Performance Requirements

Parameter	Azimuth Axis	Elevation Axis
Range (Degrees)	±90	±22.5
Quantization Level (Bits)	18	16
Angular Acceleration (rad/s2)	4-(min.) 8-(max)	2-(min.) 10-(max)
Angular Position Knowledge (µrad)	15	5
Angular Position Control (µrad)	30	18
Mirror Inertia (kg-m2)	0.006	0.006

In addition to meeting the pointing and slewing requirements for mission objectives, this gimbal had to be lightweight-(<5 kg including electronics) and compact.

3.0 DUAL-AXIS GIMBAL DESIGN

The gimbal design displayed in Figure 3 evolved from an attempt to meet the mission objectives just discussed. This section describes various features of the gimbal and the rationale for their selection.

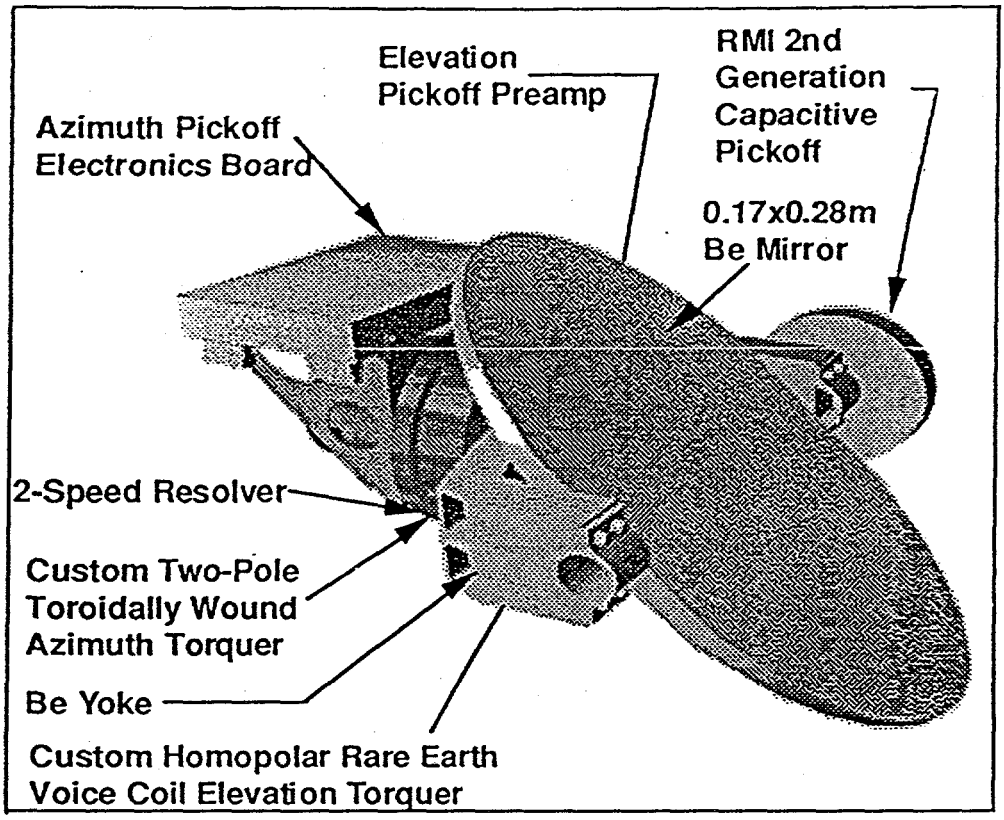

Figure 3: Dual-Axis Gimbal Design

3.1 Gimbal Material Selection

To meet the environmental, LOS pointing and overall mission requirements, the gimbal had to be lightweight and capable of conducting heat away from the polished nickel plated mirror. The low mode structural resonance of greater than 600 Hz demanded a material with a higher modulus. After careful

Table 2: Physical Properties of Common Space Materials

Material	Modulus of Elasticity (N/m^2)	Density-(kg/m^3)	Thermal Conductivity (W/m-C)	Coefficient of Thermal Expansion ($x10^{-6}C$)
Beryllium-(S200F)	$303x10^9$	$1.848x10^3$	210	11.6
T6061-Aluminum	$69x10^9$	$2.7x10^3$	202	23.2
17-4PH Stainless Steel	$207x10^9$	$8.02x10^3$	300	12

consideration of weight, stiffness, and thermal capacity, Beryllium was selected as the material for the mirror and yoke. Its properties are summarized in Table 2 against Aluminum and 17-4 Stainless Steel. As shown, Beryllium has superior stiffness-to-weight ratio and comparable thermal conductivity. By selecting the same material for the mirror and yoke, both bearings could be attached to the mirror and

the yoke without fear of thermal loading problems. The outer housing was fabricated from 17-4 Stainless Steel because its thermal coefficient of expansion was sufficiently close to Beryllium. The added inconvenience of working with Beryllium was worthwhile considering the improved performance achievable.

3.2 Gimbal Mirror

As stated above the commercial grade S200F Beryllium was also chosen as the base material for the gimbal mirror whose design is depicted in Figure 4. In this figure the elevation axis passes through the center of mass of mirror and is parallel to its minor axis. An elliptical shape provides greater area to wide FOV cameras and to distribute heat. In addition to having good stiffness-to-weight and thermal conductivity properties Beryllium also has an important use in infrared optics. At medium to long-wave infrared wavelengths, Beryllium has a reflectivity on the order of 99% of the incident intensity. This enables Beryllium to be used in many remote deep-space military applications.

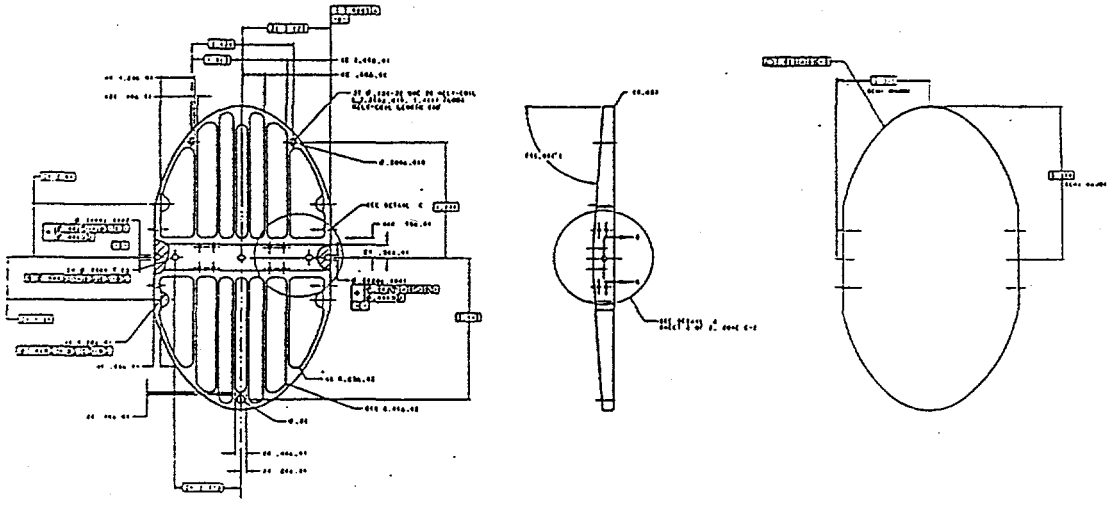

Figure 4: Gimbal Mirror Layout

3.3 Transducer Selection

Elevation Axis

A capacitive pickoff sensor was selected for angular measurement about the elevation axis because of its high resolution(~1 μradian), compact size and weight-(< 45 grams). Figure 5 displays the sensor's capacitive pickoff elements. The output voltage of the capacitive sensor is proportional to the angular displacement of the rotor relative to the fixed stator plates. The sensor linear angular range is limited to ± 22.5 degrees. This covers typical viewing scenarios for targets of interest from LEO altitudes of 400 to 700 km.

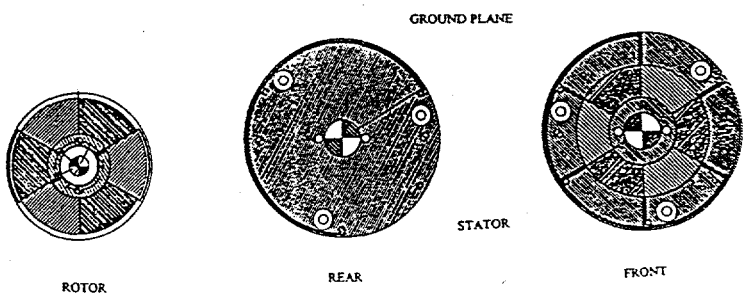

Figure 5: Elevation Axis Capacitive Pickoff Device

Azimuth Axis

A proven space qualified coarse/fine resolver was selected to measure angular motion about the azimuth axis. This unit has a high resolution, 32:1 speed, fine winding, with accuracy of 10 arcseconds. This transducer was selected based on its weight and size. It resolves over the angular range of 180 degrees of azimuth axis travel.

3.4 Actuator Selection

Elevation Axis

The elevation axis servo uses a custom IxB two magnet voice coil type actuator displayed in Figure 6. The low mass component of this actuator is the coil and is mounted to the mirror interface bracket. This mounting prevents optical distortion and reduces heat conduction to the mirror. The stator which corresponds to the larger mass element is mounted directly to the gimbal fork. The centering of the elevation axis actuator about the azimuth axis reduces the torque required by the azimuth axis servo.

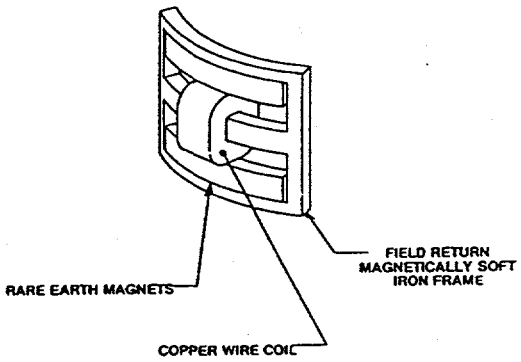

Figure 6: Elevation Axis Torquer

Azimuth Axis

The azimuth axis servo is a custom design consisting of a two pole torroidally wound brushless dc motor. This design was chosen to minimize hysterisis drag torque at the expense of weight compared to a multipole dc torquer with a stator wound on stacked laminations. Some simplicity was gained through the use of a conventional amplifier as opposed to the added electronics required to commute the windings of a multipole machine. The azimuth axis was supported using a duplexor pair of angular contact bearings at one end of the trunion axis and a single floating bearing at the other end.

3.5 Bearings

An important feature that has been incorporated into the gimbal design is the use of custom bearings for supporting the gimbal mirror. The bearings are self-aligning, exhibit low friction and provide high load capability.

3.6 Gimbal Weight Summary

The mechanical and electrical weight breakdown for all components associated with the gimbal design are summarized in Table 3. As indicated by their weight, rotating components of the azimuth axis comprise approximately 40% of the overall mechanical weight of the gimbal whereas rotating components of the elevation axis servo make up less than 18% of the overall mechanical weight. The remaining weight can be attributed to stationary parts like the azimuth axis motor stator and the support structure for mounting the gimbal to the payload optical bench. The electronics which includes pre-amplifier boards, servo control boards and power conditioning boards for the elevation and azimuth axis

respectively, contribute approximately 35% to the total weight of the gimbal. This weight reflects the development electronics and not the actual flight electronics.

Table 3: Gimbal Weight Summary

	Gimbal Part	Mass-gr	Weight-lbs
1	Mirror	583.4	1.342
2	Sum of Elevation Axis Rotating Parts	161.6	0.372
3	Sum of Azimuth Axis Rotating Parts	1694	3.896
4	Sum of Stationary Parts	1786	4.108
5	Gimbal Total Weight	4225	9.717
6	Remote Electronics	2315	5.324
	Grand Total	6540	15.042

4.0 GIMBAL SLEWING PERFORMANCE

Upon completion of the design and fabrication phase of the prototype gimbal, several laboratory tests were conducted to determine its ability to meet initial performance requirements. These tests involved calibration and responses to closed-loop step and tracking commands. To conduct these tests, a test stand was configured to mount the gimbal and a 256x256 MWIR camera (FOV = 5.57 degrees) was employed. A computer workstation served as the host for sending commands to the gimbal microprocessor and for processing digital image data from the camera. The components for this test setup are depicted in Figure 7.

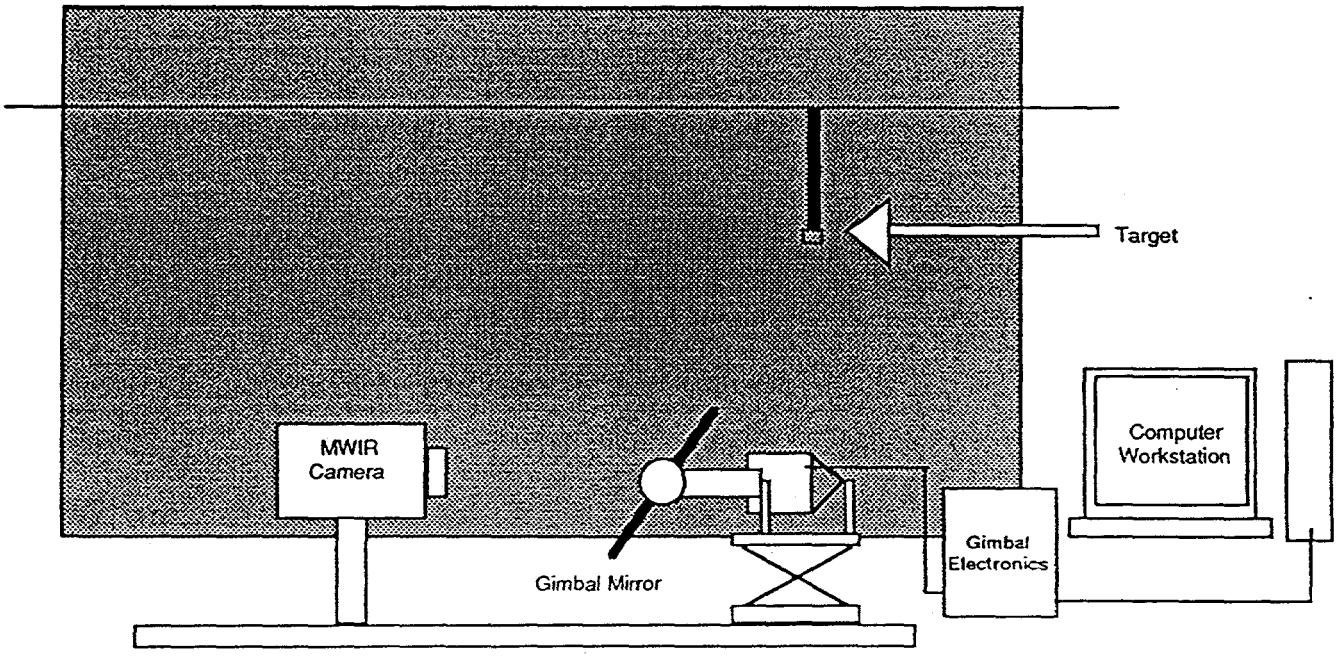

Figure 7: Test Setup for Closed-Loop Tracking Experiments

The servo control block diagrams of the elevation and azimuth axis are displayed in Figures 8 and 9 respectively. Notice that both control loops contain the option to program feedforward acceleration and

deceleration commands to maximize the performance of the servos in each axis. These feedforward commands were not used during the tracking experiments discussed in the next section.

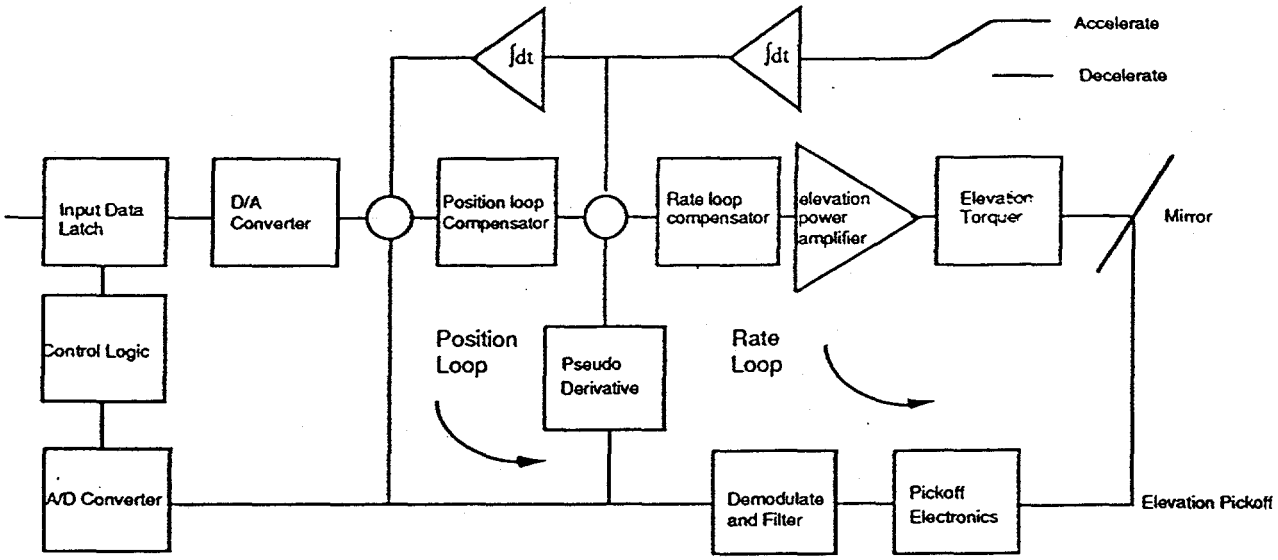

Figure 8: Elevation Block Diagram

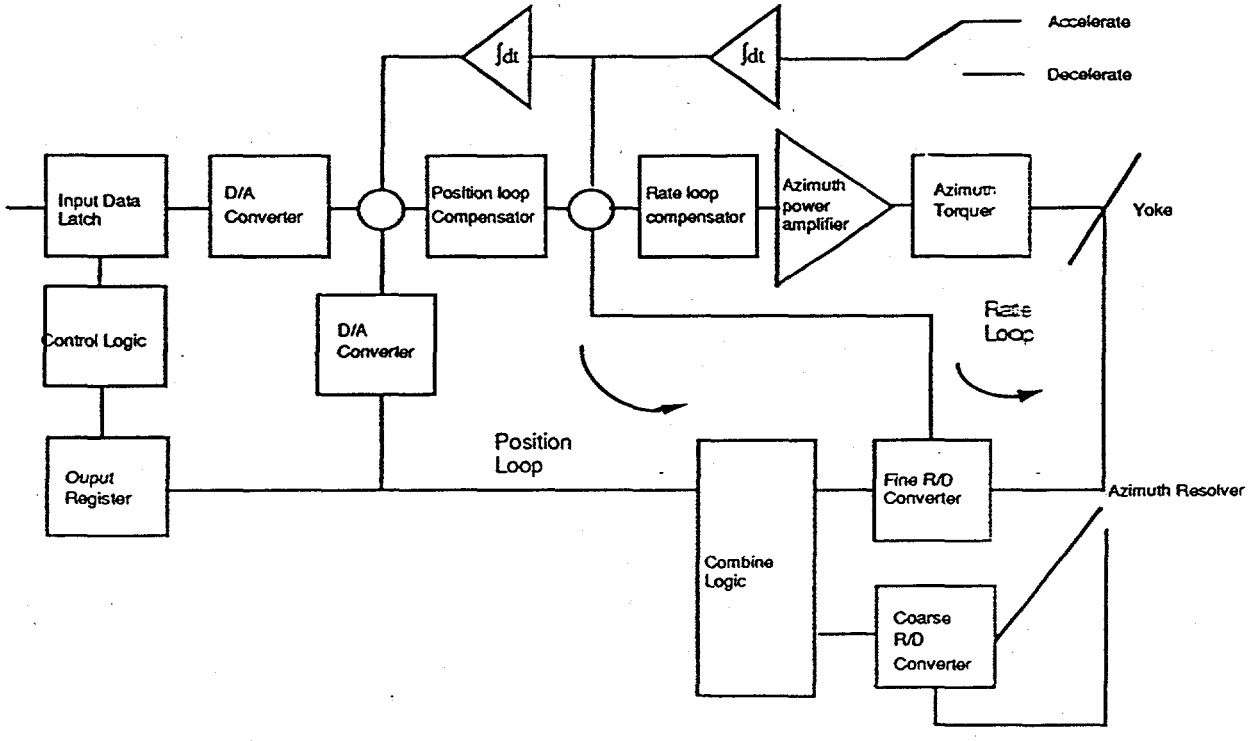

Figure 9: Azimuth Block Diagram

4.1 Step Response

To illustrate the response of the system in each axis, a step command in angle was used as input to each individual axis. The azimuth response for such a command is displayed in Figure 10 for a change in angle of 1.10 degrees. The y-axis of this plot is listed in terms of counts, where 1-count equals approximately 48 μrad which corresponds to the Quantization level of the azimuth angular range. Notice that the total step and settle time is about 0.5 seconds using this command input. There is a 50% overshoot as the azimuth servo loop attempts to track the command.

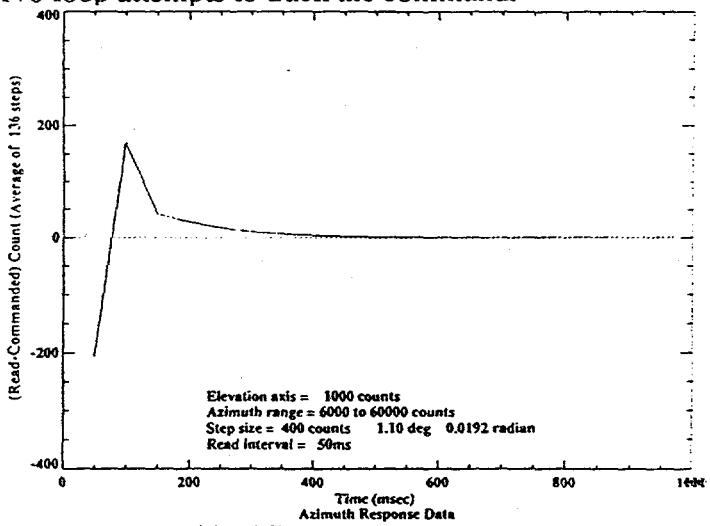

Figure 10: Step Response in the Azimuth Axis to Δ angular command of 1.10 degrees.

The elevation axis response to a step command in angle is displayed in Figure 11 below.

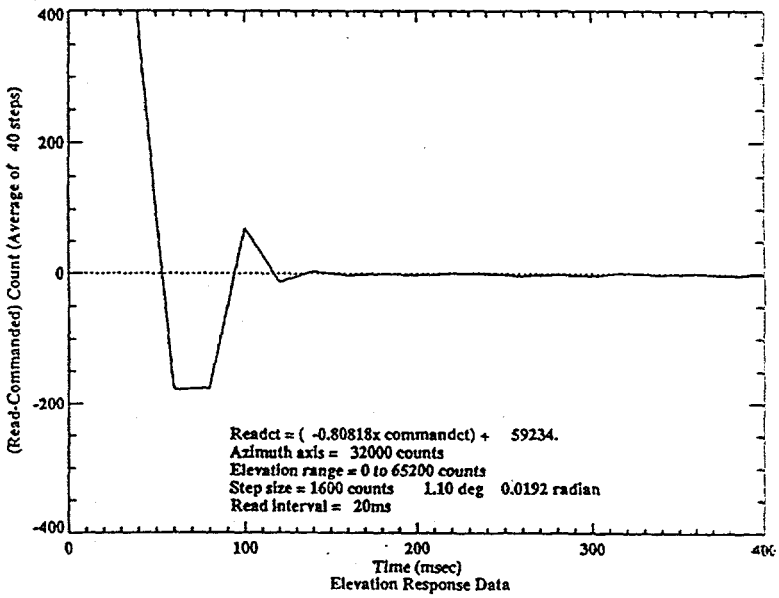

Figure 11: Step Response in the Elevation Axis to Δ angular command of 1.10 degrees.

4.2 Laboratory Target Tracking

To simulate the target tracking capability of the camera/gimbal system displayed in Figure 7, a linear rail was constructed to guide a small battery powered flashlight at a fixed elevation back and forth in front of a black background. The linear rail system was located at a height of 4 feet and a distance of approximately 20 feet from the closest point of approach to the camera/gimbal mount assembly. A variable speed DC motor was used to drive the linear motion of the flashlight via two sets of pulleys connected to the motor through a taut rope. At the maximum setting the DC motor could drive the battery powered flashlight at a speed of 2 feet/sec. At the closest point of approach this corresponded to a simulated angular rate of 0.1 rad/sec. The speed setting and target direction on the DC motor had to be manually operated and was not part of the closed-loop optical tracking system.

The 10-brightest pixel centroiding algorithm with a set threshold level was used to track images from the flashlight target at a 10 Hz rate. The gimbal was then commanded to track this hot target about the center of the camera CCD pixel array. Results from preliminary tests of this system are displayed in pixel coordinates in Figures 12 and 13 for multiple passes of the target back and forth across the black background. At the point where reversal of direction occurs, slippage of the rope drive and deceleration/acceleration of the target cause the tracking system to momentarily lose center track as the gimbal attempts to catch up with the accelerating target. At these occurrences the gimbal performs a search and relocates the target to continue tracking. Notice that further along the rail the gimbal locates and tracks the target successfully. Because the flashlight target source fills several pixels in the camera array, the gimbal track tends to jump around the array centerpoint of (128, 128).

The measured performance of the gimbal is summarized in Table 4 below. Deviations from the desired performance requirements of Section 2.0 can be attributed to the choice of a space-rated 16 bit converter for the azimuth channel in lieu of an 18 bit converter. Also the measured acceleration was lower because of the extra mass needed to protect the mirror in the laboratory environment.

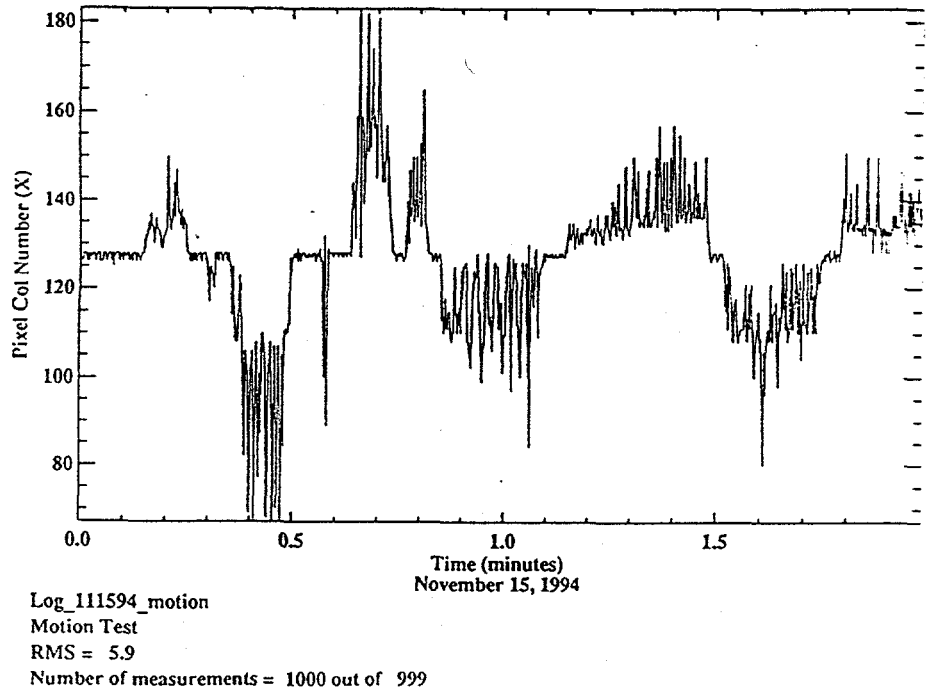

Figure 12: Target track performance in x-axis pixel coordinates of the MWIR camera.

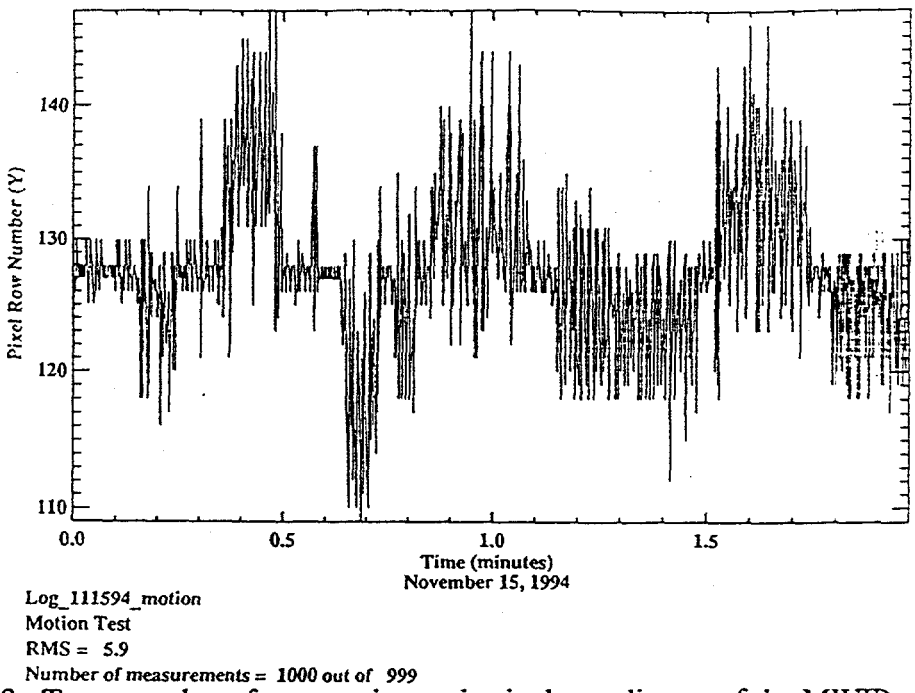

Figure 13: Target track performance in y-axis pixel coordinates of the MWIR camera.

Table 4: Measured Gimbal Performance

Parameter	Azimuth Axis	Elevation Axis
Range (Degrees)	±82.5	±22.5
Quantization Level (Bits)	16	16
Angular Acceleration (rad/s2)	1-(max)	1-(max)
Angular Position Knowledge (μrad)	48	48
Angular Position Control (μrad)	48	48
Max Slew Rate (rad/s)	0.44	0.27

5.0 SUMMARY

LLNL has developed a lightweight space-borne gimbal which can slew on demand both open loop and closed loop. The gimbal supports current TMD objectives but can also be used for other space and airborne applications. The gimbal has been operated in both search and track modes and performs adequately. Minor improvements are needed in the elevation axis to improve accuracy. Also tests on real targets which are intended to fill only a pixel of the camera would further demonstrate the performance of the system. Further laboratory tests are required to accurately characterize individual components of the gimbal.

6.0 Acknowledgments

This work was funded under contract B235364 at Lawrence Livermore National Laboratory-LLNL. The authors would like to thank Dr. Steven J. Sackett and Dr. N. J. Colella, Program Leaders in O Division at LLNL, funded by the Ballistic Missile Defense Organization-(BMDO), for continued funding for this gimbal system, Linda Ott and Eric Parker of LLNL for integration of the gimbal system into the laboratory configuration and performing many of the tracking experiments, Bill Taylor of LLNL for providing detailed mechanical design drawings of the system and Mark Jones of LLNL for providing key support in reviewing the electrical schematics.

This work was performed under the auspices of the U.S. DOE by LLNL under contract no. W-7405-Eng-48.

7.0 REFERENCES

[1] D. A. Fulghum, "Missile killing UAV Makes Initial Flights," Aviation Week & Space Technology, August 23, 1993.

[2] R. Tuttle, " Airborne Sensors draw new interest, " Aviation Week & Space Technology, January 10, 1994.

[3] E. A. Swanson and J. K. Roberge, "Design considerations and experimental results for direct-detection spatial tracking systems," Opt. Eng., 28(6), 659-666, 1989.